Rapid characterization of large volcanic eruptions: measuring the impulse of the Hunga Tonga explosion from teleseismic waves

Authors: Piero Poli[1] Nikolai Shapiro[1]

[1]ISTerre Institut des Sciences de la Terre, CNRS, Université Grenoble Alpes.

Key points

1. Hunga Tonga volcanic explosion has been automatically detected with surface waves recorded by global seismological network

2. Analysis of global surface waves resulted in measurement of the explosion impulse and led to estimating its Volcanic Explosivity Index as 6.

3. With real-time implementation of our methods, major volcanic explosion can be detected and characterized within less than 2 hours.

Abstract

Most of the largest volcanic activity in the world occurs in remote places as deep oceans or poorly monitored oceanic islands. Thus, our capacity of monitoring volcanoes is limited to remote sensing and global geophysical observations. However, the rapid estimation of volcanic eruption parameters is needed for scientific understanding of the eruptive process and rapid hazard estimation. We present a method to rapidly identify large volcanic explosions, based on analysis of seismic data. With this methodology, we promptly detect the January 15, 2022 Hunga Tonga eruption. We then analyze the seismic waves generate by the volcanic explosion and estimate important first-order parameters of the eruption. We further relate the parameters with the volcanic explosivity index (VEI). Our estimate of VEI~6, indicate how the Hunga Tonga eruption is among the largest volcanic activity ever recorded with modern geophysical instrumentation, and can provide new insights about the physics of large volcanoes.

Plain language summary

The Hunga Tonga volcanic eruption that occurred on January 15, 2022 had a global impact with ejecting a huge amount of ashes and volcanic gases in the atmosphere and with generating tsunami that affected many Pacific countries. This volcanic event has been also well recorded by modern satellite and land based geophysical instruments. Despite of the unprecedented wealth of high quality and rapidly available scientific data, main quantitative parameters of the Hunga Tonga volcanic eruption such as its size in comparison with previous major eruption could not be estimated rapidly with "standard" monitoring algorithms. This emphasize the need to develop new approaches for analysis of instrumental observations. We show how the data recorded by seismographic stations operating all around the World which are available in real time can be analyzed to determine main eruption parameters including its location and size within less than two hours after its occurrence.

Introduction

Despite the development of volcano observatories in many countries, most of potentially active volcanoes (whose exact number is not well defined; Global Volcanism Program, 2013, https://www.usgs.gov/faqs/how-many-active-volcanoes-are-there-earth) can be monitored only remotely based on satellite observations (e.g. Vaughan & Webley, 2012) and global network of geophysical instruments. The recent Hunga Tonga catastrophic eruption perfectly

illustrated this situation. This event occurred on January 15, 2022 on a small uninhabited and unmonitored volcanic island. Its impact, however, was truly global. The volcanic explosion ejected an enormous ash plume well recorded by satellites and significantly affecting the Tonga islands, generated a very strong atmospheric pressure wave recorded by meteorological and infrasound sensors across the World, and was followed by a well recorded tsunami that affected many Pacific coastal regions (Duncombe, 2022).

Based on information available today the Hunga Tonga explosion is most likely to be the largest one occurred in the 21-st century (Duncombe, 2022), but still, despite the large amount of observations available, a full quantitative estimation of the size of this eruption remains challenging to obtain rapidly.

Quantifying the size and strength of volcanic eruptions is a difficult task because of their strongly varying styles and poor available data for many past eruptions. The widely used parameter in volcanology is the Volcanic Explosivity Index (VEI) that is a logarithmic scale based on estimations of volumes of erupted materials (Newhall and Self, 1982). The VEI scale allowed to build a quantitative catalog that includes many historical and pre-historical eruptions (Newhall and Self, 1982; Mason et al., 2004). Extending this catalog back in time is very important for statistical analysis because of very rare occurrence of largest eruptions (VEI≥5).

The VEI scale has its inconvenience from the point of view of real time monitoring because estimating volumes of erupted materials remains relatively slow, as can be seen with the Hunga Tonga eruption. At the same time, today's strong volcanic eruptions are recorded by satellites and hundreds of high-quality geophysical instruments distributed all over the World. An efficient usage of these data for global-scale real-time volcanic monitoring requires developing instrument-based scale of the size of eruptive phenomena, similar to magnitudes or seismic moments routinely determined for earthquakes. Ideally, such an "eruption magnitude" scale should be based on a plausible physical model of the eruptive process (source) and cold be linked with widely used VEI scale.

Because of the very variable style of volcanic eruptions, a universal physical model of the eruption processes is not possible. Here we focus on most dangerous strong explosive eruptions. The waves emitted by these events are well recorded by global networks of seismic and infrasound stations. The latter are particularly energetic because of the strong coupling of volcanic explosions with the atmosphere and, therefore, have been used to model volcanic explosion source process (e.g., Matoza et al., 2011; Haney et al., 2018) and to estimate eruptive volumes (e.g., Fee et al., 2017). Acoustic coupling with the ionosphere also can be used for volcano monitoring (e.g., Manta et al., 2021). One of the main difficulties with the infrasound monitoring of the eruptions is the need to correct for non-stationary propagation effects strongly dependent on atmospheric winds (e.g., Le Pichon et al., 2005). Atmospheric acoustic waves are also relatively slow and several hours are required to record a representative dataset from a global network (see Fig S3).

On the contrary, seismic waves propagation is stable in time and rather fast. Surface waves from large volcanic explosions (and body waves for the strongest ones) are regularly recorded and data from hundreds of stations can be collected within an hour following the eruption. This makes seismic networks one of the most suitable tools for the real-time monitoring of volcanic explosions and determining their physical characteristics (e.g., Zobin et al., 2006; Prejean and Brodsky, 2011). At the same time, "standard" seismological methods and metrics developed for earthquake monitoring are not applicable to volcanic eruptions. First, the latter do not emit strong high-frequency body waves that are used in most of earthquake detection algorithms. Second, the earthquake magnitude and moment scales are not applicable to volcanic explosions because of different frequency ranges and because of the fundamentally different source mechanism.

In this short paper, we show how a fast analysis based on backprojection of long-period surface waves recorded by the global seismic network (e.g., Ekström, 2006; Poli 2019) could be used to detect the Hunga Tonga explosion nearly in real time and to determine its geographical location. We then use a model describing the mechanical effect of volcanic eruption as a single force (Kanamori and Given, 1982; 1984, Nisimura, 1995) to deconvolve the propagation effect in order to estimate the source force spectra that, in turn, can be used to approximately estimate the overall mechanical impulse of the explosion (Volcanic Explosion Impulse: VEIm) and its duration. We than use the volcanic jet model (Brodski et al., 1999; Prejean and Brodsky, 2011) to estimate the total ejected mass and link it to the Volcanic Explosivity Index, VEI. Overall, the implemented seismic data analysis provides a realistic and physics-based workflow for real-time monitoring of large volcanic eruptions.

Detection of long period events

From the time continuous analysis of long period surface waves (Poli, 2019), recorded at global seismic stations (Fig. 1a), we detected a new event, on Saturday 15 of January 2022 (UTC 04h16m00.07s), with location close to the Tonga Islands, as showed in the map of back-projected signals in Figure 1a and b. This event was rapidly associated with a major volcanic eruption of the Hunga Tonga, announced by many medias.

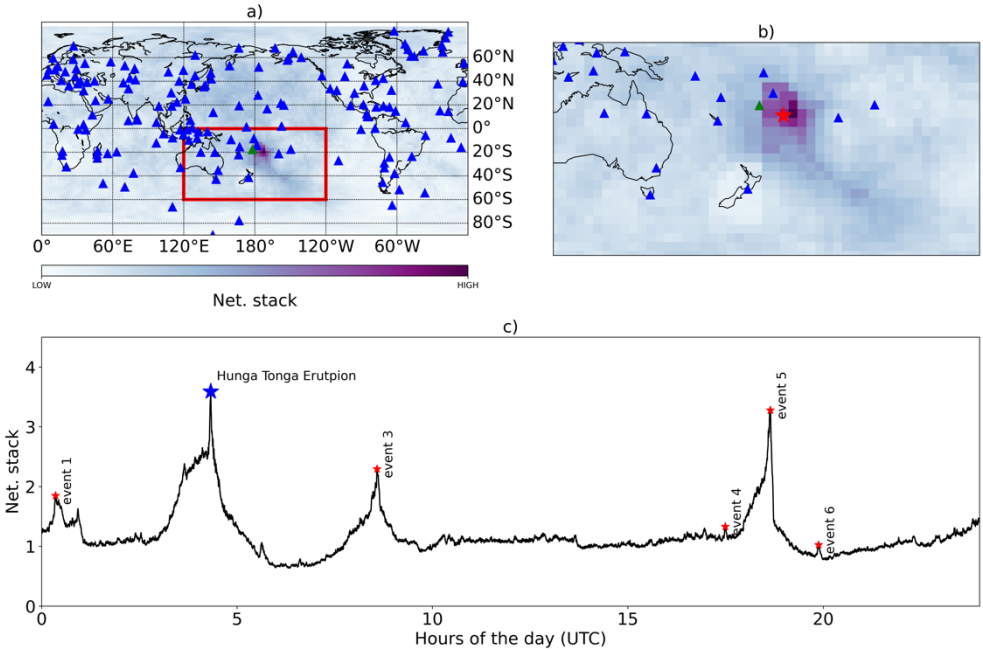

Figure 1: *a) Map showing the seismic stations used in this study (blue triangles) and the network stack at the Hunga Tonga event time. The green triangle is a reference station used to plot the spectrum of recorded signal in figure 2b. The red polygon encloses the source region plotted in b). The red stat in b is the position of the Hung Tonga volcano. c) Network stack for the 15 of January 2022, with detected signals represented by red stars. The blue star it the detection associate with the Hunga Tonga eruption.*

The detection algorithm is similar to Shearer (1994) and Poli (2019), (see also Ekstrom, 2006), and is based on the analysis of 24 hours seismograms recorded by seismic networks II (Scripps Institution of Oceanography, 1986), IU (Albuquerque Seismological Laboratory (ASL)/USGS, 1988), GE (GEOFON Data Centre, 1993) and G (Institut de physique du globe de Paris (IPGP), & École et Observatoire des Sciences de la Terre de Strasbourg (EOST), 1982, Fig. 1a, blue stars), resampled at 0.1Hz and corrected for the instrumental response. Only long

period and vertical components channels are used (LHZ and VHZ), and data are filtered in between 0.01 and 0.03Hz. Similar to Shearer (1994) each seismogram is then transformed into STA/LTA time series, using a recurrent scheme (Whiters et al., 1998) with STA=120s and LTA=900. We then assume equally spaced sources every 2.5deg, located at the surface of the Earth. For each source, we align the seismograms assuming a velocity of 3.85Km/s, derived from PREM (Dziewonski & Anderson, 1981), and stack all the seismograms. For every time sample the stacked signal at each source position is saved. The maxima of the stacked signal as function of time define the network stack (Fig. 1c), from which we extract events, as local maxima with prominence larger than 0.2 and interspaced by at least 3600s. These parameters have been arbitrary chosen after many tests, to minimize the incidence of false detections, while favoring detection of small size events.

Detection are associated with known earthquakes, if a seismic event of magnitude larger than 3 (ISC catalog, Storchak et al., 2013) occur within 10deg and 3600 seconds from the time and position of our detection. Otherwise the detection is flagged as a new event. The detection runs automatically every day, at 5am (UTC+1) on a desktop computer and takes ~5min. Every day an event report is produced with known earthquakes and new events.

Figure 1a and b shows the distribution of the network stack for each tested source position at the time of the event (15 of January 2022 UTC 04h16m00.07s), with the violet areas representing the most likely location of the discussed event. Beyond the Hunga Tonga event, on the 15 of January 2022, 5 additional detections are present (Fig. 1c), 3 of which are associated with known earthquakes, while the other 2 are, a long period event in the Pacific Antarctic ridge, and a possible glacial event in East Antarctica (see supplementary materials).

The waveforms for the Hunga Tonga event are plotted in Figure 2, and show a good alignment when ranged as function of distance from the source, proving the quality of our location. The dominant signals are Rayleigh waves (Fig. 2), with several impulses likely to represent explosion episodes as for the mount St. Helens eruption in 1980 (Kanamori & Given, 1982, Brodsky et al., 1999). The Rayleigh waves train last for ~6000s, a time which can be taken as an approximated estimation of the duration of the eruption. Before the arrival of surface waves, more rapid S and P waves are also observed (Fig. 2).

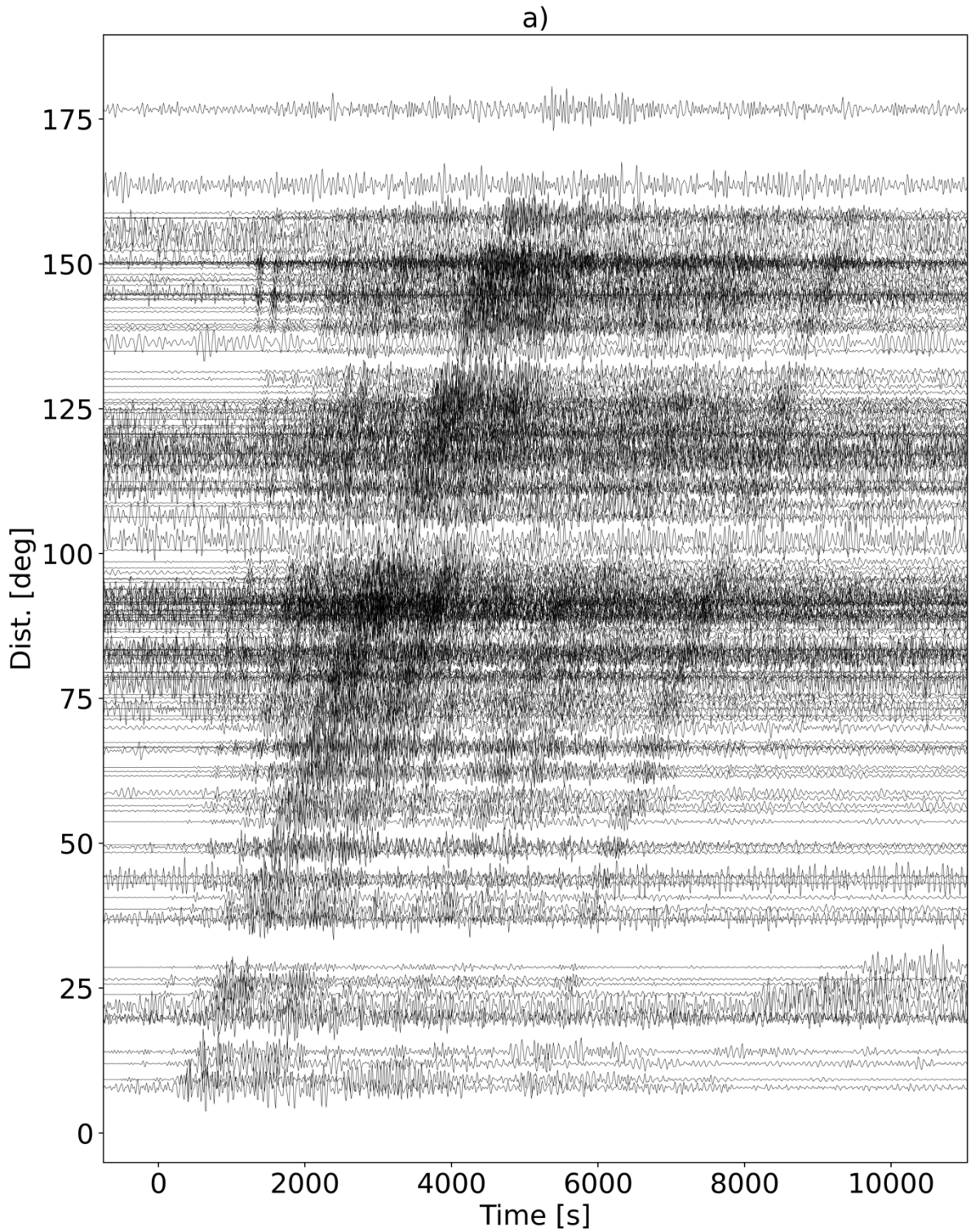

Figure 2: *a) Signals generated by the Hunga Tonga eruption, recorded at stations of the global seismographic network reported in Fig. 1a, plotted as function of distance from the source. Each trace is normalized by its absolute maximum and filtered in between 0.01 and 0.04Hz.*

Impulse of the explosive eruption

The seismic radiation of large volcanic explosions can be approximated with a response to a reaction force acting on the ground in the direction opposite to the motion of the ejected ash column (e.g., Kanamori & Given, 1982, Nishimura, 1995; Cruz-Atienza et al., 2001).

Therefore, the far field seismic wavefield can be expressed as a convolution of the single force with the Green's function:

$$u(t,r) = F(t) * G(t - t_s, r, r_s) \quad [1]$$

where *u(t,r)* is the displacement observed in location *r*, r_s and t_s are location and origin time of the explosive eruption, *G* is the Green's function, and *F(t)* is time variable force acting as the eruption source. Equation (1) implies that given sufficiently broadband records available at several stations and azimuths, a full vector force time history can be retrieved via convolution or inversion procedures (e.g., Kanamori & Given, 1982, Cruz-Atienza et al., 2001; Allstadt, 2013).

To simplify the rapid data analysis, we consider an approximation of a vertical explosion and force, which is plausible at first order considering the nearly radially symmetric shape of the Hunga Tonga ash cloud seen by satellites. In this case, the vertical displacement can be written as:

$$u_z(t,r) = F_z(t) * G_{zz}(t - t_s, r, r_s) \quad [2]$$

where F_Z is vertical forces and G_{zz} are the vertical component of the Green's function for a vertical force at the source. Again, the full force time history $F_z(t)$ can be retrieved by applying a deconvolution of equation (2) to the data. The spectral representation of the source force $F_z(\omega)$ is computed with a Fourier transform:

$$F_z(\omega) = \int F_z(t) e^{-i\omega t} dt \quad [3]$$

If the explosion time history $F_z(t)$ is positively defined its Fourier spectrum $F_z(\omega)$ will converge at low frequencies to a "plateau":

$$\lim_{\omega \to 0} F_z(\omega) = \int F_z(t) dt = K_0 \quad [4]$$

and if it can be approximated with a single unidirectional pulse of duration τ_{exp}, the amplitude falls down above the corner frequency f_c approximately inverse to the explosion duration:

$$f_c \approx 1/\tau_{exp} \quad [5]$$

There is a clear similarity with the low-frequency asymptotic behavior of the classical earthquake spectra (e.g., Brune 1970, Kanamori & Given, 1982). The main difference is that the seismic moment M_0 is replaced with the value K_0 that is equal to the total explosion impulse (e.g., Nishimura, 1995; Cruz-Atienza, 2001). Therefore, similar to the analysis of earthquake, two main parameters of volcanic explosion K_0 and f_c can be determined from the analysis of the source amplitude spectra (Kanamori & Given, 1982). This implies that we do not need to compute a full deconvolution of equation (2) and can use its amplitude version in the Fourier domain:

$$|u_z(\omega)| = |F_z(\omega)||G_{zz}(\omega)| \quad [6]$$

to retrieve the amplitude source spectra $|F_z(\omega)|$ from simple spectral ratios.

To estimate the source spectrum, we use the data shown in Fig. 2a. At this stage, we do not down sample the seismograms and bandpass them between 0.0001 and 0.1Hz, and

converted into displacement by removing the instrument responses. The vertical component Green's functions for a vertical force is obtained from the "syngine" data service (Hutko et al., 2017) based on the PREM model (Dziewonski & Anderson, 1981). We then use equation (6) and calculate the spectral ratio between the recorded signals and the Green's functions, to estimate the source spectrum $|F_z(\omega)|$ for the Hunga Tonga eruption. The spectral ratios are calculated for each station using the and the full duration of the eruption, that is 6000s following the arrival times of Rayleigh waves, calculated from PREM. This window is chosen to avoid interference with the long period and strong amplitude signals, for atmospheric acoustic waves, well recorded by seismic stations (see Fig. S3).

Before calculation of the spectral ratio (equation 6) we estimate the signals to noise ratio (SNR) for each spectrum. The SNR is defined as the ratio of the amplitude spectrum for the surface waves and 1 hour of signal preceding the eruption. Only frequencies with SNR > 10 are retained for further analysis.

The final force spectrum is the average of single station force (blue line Fig. 3a), while the data error is the standard deviation of the 41 single station force spectra (blue area, Fig. 3a). The force spectrum shows a low frequency spectral "plateau" for frequency lower than 5mHz, which is used to estimate the explosion impulse (equation 4): $K_0 \approx 1.3\ 10^{15}\ Ns$. The spectrum starts to fall-off at a corner frequency $f_c \approx 0.005\ Hz$, suggesting an approximate explosion duration of ~200s (equation 5). We cannot exclude a possibility that the obtained value of K_0 might be underestimated (and f_c overestimated) because of the limited signal-to noise ratio at very slow frequencies. These values have therefore to be considered as a lower bound estimates of the full eruption size and duration.

We further estimate the force spectrum for well recorded P waves. We only focus on the frequency range from 0.01 to 0.07Hz, where signal to noise ratio of the P waves is suitable for our analysis. We then isolate 200s of signal, around the P waves arrival time estimated from PREM model (Dziewonski & Anderson, 1981). We use again equation (6) to estimate the force for the signals recorded at 42 stations. The average force spectrum from P waves (black line in Fig. 2a) is remarkably similar to the one from Rayleigh waves at frequencies above 0.01 Hz. We also note that the spectral fall-off above the corner frequency is not "homogeneous" with appearance of a second plateau between 0.01 and 0.04 Hz. This implies that, if we would make "rapid" estimations based on P-waves or on relatively high-frequency Rayleigh waves (as those used for the backprojection shown in Figs 1 and 2) we would obtain $K_0 \approx 2\ 10^{14}\ Ns$ and a corner frequency close to 0.04 Hz. This observation, together with the shape of the amplitude source spectrum (Fig. 3a) indicates that the eruption force time function F(t) is most likely composed of several pulses with different durations (which would explain the existence of two spectral plateaus) and that the analysis of only P waves (or band-limited surface waves) does not capture the full impulse of the eruption but only its relatively short-time scale component. However, such analysis can be still useful to obtain provide a rapid lower bound estimate of the explosion impulse (Fig. 3a) and total ejected mass (dashed black line in Fig. 3b)

Relationship between the volcanic explosion impulse, the erupted mass and volume, and the Volcanic Explosivity Index, VEI

Our analysis suggests that the explosion impulse K_0 is the parameter that can be directly and robustly estimated for large explosive eruptions, from a simple and fast analysis of broadband seismic records. It is also a natural dynamic parameter characterizing the explosions similar to seismic moment characterizing the earthquakes. Therefore, the volcanic explosion impulse could be considered as a cornerstone for building instrument based scales of the size of volcanic eruptions. At the same time, this is important to link this parameter with other existing seismological and vulcanological scales.

From seismological point of view, determinations of K_0 could lead to developing a physical seismic magnitude scale as has been suggested by Cruz-Atienza et al. (2001). Based on analogy with the moment magnitude scale for earthquakes, the relationship between the magnitude M and the explosion impulse should be written as $M=2/3 \log K_0+C$, where the constant C should be calibrated to approximately fit "standard" magnitude estimations. However, such calibration is beyond the scope of this study.

As described in the introduction, the main scale used in volcanology is the Volcanic Explosivity Index (VEI) that is a logarithmic scale based on estimations of the erupted volume (Newhall and Self, 1982). The latter can be approximately estimated from the explosion impulse, assuming a value erupted material density and a simple physical model for the volcanic explosion. In particular, we use the model of Brodsky et al. (1999) in which the reaction force from the explosion is described as a jet force F_{jet}. For simplification, we consider an eruption with a constant jet velocity V_{jet}, leading to the jet force being proportional to the mass discharge rate:

$$F_{jet}(t) = V_{jet}\dot{m}(t) \quad [7]$$

By combining (4) and (7) we find a simple equation to estimate the total eject mass ($m_{total} = \int \dot{m}\, dt$):

$$m_{total} = K_0/V_{jet} \quad [8]$$

We consider the possible range of jet velocities between 200 and 570 m/s, as suggested by Brodsky et al., (1999) to estimate the total mass estimation shown in Fig. 3b. In particular, the estimation based on the lower bound of V_{jet} is: $m_{total} \approx 1.3\ 10^{13}\ kg$.

The next step is to use an average tephra density (ρ_{tephra}) to convert the erupted mass into volume:

$$V_{total} = m_{total}/\rho_{tephra} \quad [9]$$

VEI is a discrete scale logarithmically related to erupted tephra volume (Table 1 from Newhall and Self, 1982). Its continuous equivalent can be written as a following equation:

$$VEI = \log\left(V_{total}/10^9\right) + 5 \quad [10]$$

where V_{total} is the volume in m^3. A final relationship between VEIm and VEI can be written as:

$$VEI = \log\left(K_0/V_{jet}/\rho_{tephra}\right) - 4 \quad [11]$$

Based on our estimation of K_0 from the broadband seismograms and with using V_{jet} = 200 m/s (Brodski et al., 1999), and ρ_{tephra}=1000 kg/m^3 (Takarada and Hoshizumi), we obtain the value of VEI of 5.8 for the Hunga Tonga eruption.

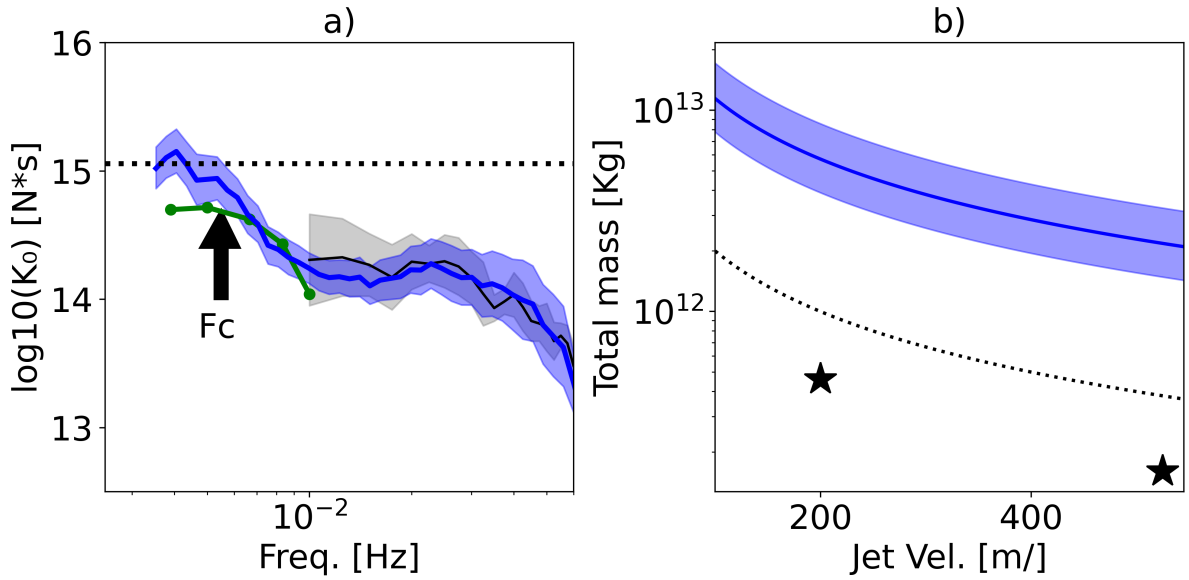

Figure 3. *a) Source spectrum obtained from the deconvolution described in eq. 6 (continuous blue line) and its confidence bound (blue area). The black line and grey area are the same estimated using P waves. The arrow indicates the estimated corner frequency (f_c) and the dashed line shows the estimated volcanic explosion impulse ($K_0 = 1.3\ 10^{15}$). We also report in green the estimated (nearly horizontal) force spectrum for the Mt. St. Helens, 1980 eruption (Kanamori & Given, 1982). b) Total ejected mass as function of jet velocity (blue line) and its uncertainty (blue area). The stars are the total ejected mass and assumed jet velocity for the 1980 Mt St Helens eruption estimated by Brodksy et al., (1999). The dashed line is the estimated ejected mass using only P waves.*

Discussion and Conclusions

We first show how the continuous analysis of long period wavefield at global scale, can help to rapidly identify and locate signals different from regular earthquakes (Figures 1 and 2). Our algorithm, which is inspired on previous works (Shearer,1996 and Ekstrom, 2006), permitted the rapid identification and characterization of the Hunga Tonga eruption.

We then used the seismic waves emitted from the source to get first order-dynamic parameters for this eruption. From the detected signals (Fig. 2a), we can qualitatively infer a long (~6000s) eruption episode, dominated by a series of explosions, similar to the Mt St. Helens 1980 eruption (Kanamori & Given, 1982, Brodsky et al., 1999). With a simple spectral ratio method (Nishimura, 1995) we estimated broadband amplitude source force spectrum (Fig. 3a). The source force spectrum at low-frequencies, clearly stabilizes at a "plateau", whose level is equal to the volcanic explosion impulse, or the integral of the vertical force in time, and takes values of $1.3\ 10^{15}$ Ns. This value is ~2.5 times larger than the estimate of Kanamori and Given (1982) for the Mount St Helens eruption (Fig. 3a). From the estimated explosion impulse, and assuming an eruption model (Brodsky et al., 1999) we obtain as estimates of the total eject mass of $1.3\ 10^{13}$ *Kg* for a jet velocity of 200m/s (eq. 4), which is significantly larger than the 1.6-4.6 10^{11} Kg, estimated by Brodsky et al., (1999) for the mount St Helens eruption in 1980.

From the analysis of the shape of the force spectrum we observe a fall-off above the corner frequency $fc \approx 0.005$ *Hz*. Corner frequencies have been observed for smaller volcanic explosions (Nishimura, 1995), and can be interpreted to be inversely proportional to the duration of the explosion. For the Hunga Tonga eruption, the ~200s duration, is likely to reflect the time extent of each explosion composing the eruption.

The compilation of f_c for several small eruptions, shows a scaling relationship between force and duration of the eruptions (Nishimura, 1995, Cruz-Atienza et al., 2001, Zobin et al., 2009). For single explosion force, and the scaling of Zobin et al. (2009) we would expect the duration of ~200s for the force of Hunga Tonga explosion, which agrees with the observed Fc~0.005Hz (Fig. 2a). Our estimated duration is longer (~200s) then ~75s estimated by

Kanamori et al. (1984) for the Mt St Helens eruption, using a similar approach. From the duration of the latter eruption (Kanamori & Given, 1982), Brodsky estimated a mass discharge rate of ~2-6e9Kg/s. With our estimates, we obtain significantly larger discharge rate, up to 6.5e10 Kg/s, Hunga Tonga eruption. However, the time window for the analysis is 6000s, thus assuming the volume is ejected along the analyzed window, we obtain a mass discharge of ~2.1e9Kg/s, more similar to the results of Brodsky et al. (1999).

We further observe how the force spectrum (Fig. 2a) stops to decay at ~8mHz, where a second plateau is observed, before an additional corner frequency at ~0.04Hz, well seen form P waves (Fig. 2a). This shape might be controlled by the eruption dynamics, and could imply explosions of variable force and duration. To test this hypothesis, we estimated the force for only the first impulse (1000s time window for surface waves, Fig. S4). This first part of the eruption lacks the long period and large amplitude force (Fig. 2a) and results in K_0 approximately ten times smaller than the one for the 6000s window, but still capture the large size of the eexplosion with a VEI up to 5.

We further relate the estimates discussed above with the volcanic explosivity index, making limited assumptions. Our analysis shows that the Hunga Tonga eruption has VEI=6, much larger than previous volcanic explosion at this volcano (Vaughan & Webley, 2010, VEI=2, from satellite data), and making it among the biggest volcanic eruption ever recorded with modern geophysical instrumentation.

An important approximation that we implemented for simplicity and robustness of the analysis is that we assume the total force being only vertical (neglecting the horizontal components). Any contribution of horizontal force will result in the underestimation of the total force, resulting in a reduced estimate of the total mass. However, assuming any horizontal force as large as 40% of the vertical force (Kanamori & Given, 1982, Cruz-Atienza et al., 2001), the final difference will be as small as ~10%. Another possible source of uncertainty is the limited signal-to-noise ratio of seismic signals at very low frequencies that might result in underestimation of the level of the low-frequency spectral plateau. With these different sources of uncertainties in mind, the presented value of K_0 should be considered as a lower-bound estimation.

To conclude, we presented a simple framework to rapidly detect and characterize remote and large volcanic eruption from the sole seismological data. The analysis of the data does not require huge computations and can be done in real time. This implies that with the described approach and with a limited set of assumptions the easily available seismological observations can be used for a rapid (within an hour) quantitative estimation of the size of large volcanic explosions (e.g. VEI). Application of this approach to the Hunga Tonga eruption suggest that it has VEI of 6.

Acknowledgements

PP and NS received funding from the European Research Council (ERC) under the European Union Horizon 2020 Research and Innovation Programme (grant agreements, 802777-MONIFAULTS and 787399-SEISMAZE, respectively).

Open Research

Seismological data and Green's function are available through the IRIS Data Management Center (IRISDMC) at http://service.iris.edu/fdsnws/dataselect/1/ and can be obtained using the IRIS DMC FDSNWS web service.

Bibliography

Albuquerque Seismological Laboratory (ASL)/USGS. (1988). *Global Seismograph Network - IRIS/USGS* [Data set]. International Federation of Digital Seismograph Networks. https://doi.org/10.7914/SN/IU

Allstadt, Kate. "Extracting source characteristics and dynamics of the August 2010 Mount Meager landslide from broadband seismograms." *Journal of Geophysical Research: Earth Surface*118.3 (2013): 1472-1490.

Brodsky, Emily E., Hiroo Kanamori, and Bradford Sturtevant. "A seismically constrained mass discharge rate for the initiation of the May 18, 1980 Mount St. Helens eruption." *Journal of Geophysical Research: Solid Earth* 104.B12 (1999): 29387-29400.

Brune, J. N. (1970), Tectonic stress and the spectra of seismic shear waves from earthquakes, *J. Geophys. Res.*, 75(26), 4997– 5009, doi:10.1029/JB075i026p04997.

Cruz-Atienza, V.M., J.F. Pacheco, S.K. Singh, N.M., Shapiro, C., Valdés, C., and A. Iglesias (2001). Size of Popocatépetl volcano explosions (1997–2001) from waveform inversion. *Geophysical Research Letters*, 28, 4027-4030.

Duncombe, J. (2022), The surprising reach of Tonga's giant atmospheric waves, *Eos, 103,* https://doi.org/10.1029/2022EO220050. Published on 21 January 2022.

Dziewonski, Adam M., and Don L. Anderson. "Preliminary reference Earth model." *Physics of the earth and planetary interiors* 25.4 (1981): 297-356.

Efron, Bradley, and Robert J. Tibshirani. *An introduction to the bootstrap*. CRC press, 1994.

Ekström, Göran. "Global detection and location of seismic sources by using surface waves." *Bulletin of the Seismological Society of America* 96.4A (2006): 1201-1212.

Fee, D., P. Izbekov, K. Kim, A. Yokoo, T. Lopez, F. Prata, R. Kazahaya, H. Nakamichi, and M. Iguchi (2017). Eruption mass estimation using infrasound waveform inversion and ash and gas measurements: Evaluation at Sakurajima Volcano, Japan. *Earth and Planetary Science Letters*, 480, 42-52, https://doi.org/10.1016/j.epsl.2017.09.043.

GEOFON Data Centre. (1993). *GEOFON Seismic Network*. Deutsches GeoForschungsZentrum GFZ. https://doi.org/10.14470/TR560404

Global Volcanism Program, 2013. Volcanoes of the World, v. 4.7.6. Venzke, E (ed.). Smithsonian Institution. Downloaded 27 Feb 2019. https://doi.org/10.5479/si.GVP.VOTW4-2013

Haney, M. M., Matoza, R., Fee, D., & Aldridge, D. F. (2018). Seismic equivalents of volcanic jet scaling laws and multipoles in acoustics. *Geophysical Journal International*, **213**(1), 623– 636. https://doi.org/10.1093/gji/ggx554

Hutko, A. R., M. Bahavar, C. Trabant, R. T. Weekly, M. Van Fossen, T. Ahern (2017), Data Products at the IRIS-DMC: Growth and Usage, Seismological Research Letters, 88, no. 3, https://doi.org/10.1785/0220160190.

Institut de physique du globe de Paris (IPGP), & École et Observatoire des Sciences de la Terre de Strasbourg (EOST). (1982). *GEOSCOPE, French Global Network of broad band seismic stations*. Institut de physique du globe de Paris (IPGP), Université de Paris. https://doi.org/10.18715/GEOSCOPE.G

Kanamori, Hiroo, and Jeffrey W. Given. "Analysis of long-period seismic waves excited by the May 18, 1980, eruption of Mount St. Helens—A terrestrial monopole?." *Journal of Geophysical Research: Solid Earth* 87.B7 (1982): 5422-5432.

Kanamori, Hiroo, Jeffrey W. Given, and Thorne Lay. "Analysis of seismic body waves excited by the Mount St. Helens eruption of May 18, 1980." *Journal of Geophysical Research: Solid Earth*89.B3 (1984): 1856-1866.

Le Pichon, A., Blanc, E., Drob, D., Lambotte, S., Dessa, J. X., Lardy, M., Bani, P., and Vergniolle, S. (2005), Infrasound monitoring of volcanoes to probe high-altitude winds, *J. Geophys. Res.*, 110, D13106, doi:10.1029/2004JD005587.

Manta, F., Occhipinti, G., Hill, E. M., Perttu, A., Assink, J., & Taisne, B. (2021). Correlation between GNSS-TEC and eruption magnitude supports the use of ionospheric sensing to complement volcanic hazard assessment. Journal of Geophysical Research: Solid Earth, 126, e2020JB020726. https://doi. org/10.1029/2020JB020726

Mason, B.G., Pyle, D.M. & Oppenheimer, C. The size and frequency of the largest explosive eruptions on Earth. Bull Volcanol 66, 735–748 (2004). https://doi.org/10.1007/s00445-004-0355-9.

Matoza, R. S., Le Pichon, A., Vergoz, J., Herry, P., Lalande, J. M., Lee, H. I., et al. (2011). Infrasonic observations of the June 2009 Sarychev Peak eruption, Kuril Islands: Implications for infrasonic monitoring of remote explosive volcanism. *Journal of Volcanology and Geothermal Research*, *200*(1–2), 35–48. https://doi.org/10.1016/j.jvolgeores.2010.11.022

Newhall, C. G., and Self, S. (1982), The volcanic explosivity index (VEI) an estimate of explosive magnitude for historical volcanism, J. Geophys. Res., 87(C2), 1231– 1238, doi:10.1029/JC087iC02p01231.

Nishimura, Takeshi. "Source parameters of the volcanic eruption earthquakes at Mount Tokachi, Hokkaido, Japan, and a magma ascending model." *Journal of Geophysical Research: Solid Earth*100.B7 (1995): 12465-12473.

Poli, Piero. "In between known earthquakes: Characteristics long period earthquakes from oceanic ridges and ultra-low frequency volcanic tremors." *Geophysical Research Abstracts*. Vol. 21. 2019.

Prejean, S. G., and E. E. Brodsky (2011), Volcanic plume height measured by seismic waves based on a mechanical model, J. Geophys. Res., 116, B01306, doi:10.1029/2010JB007620.

Scripps Institution of Oceanography. (1986). *Global Seismograph Network - IRIS/IDA* [Data set]. International Federation of Digital Seismograph Networks. https://doi.org/10.7914/SN/II

Shearer, Peter M. "Global seismic event detection using a matched filter on long-period seismograms." *Journal of Geophysical Research: Solid Earth* 99.B7 (1994): 13713-13725.

Storchak, Dmitry A., et al. "Public release of the ISC–GEM global instrumental earthquake catalogue (1900–2009)." *Seismological Research Letters* 84.5 (2013): 810-815.

Takarada S. and H. Hoshizumi (2020). Distribution and Eruptive Volume of Aso-4 Pyroclastic Density Current and Tephra Fall Deposits, Japan: A M8 Super-Eruption. *Frontiers in Earth Science*, 8, DOI:10.3389/feart.2020.00170.

Vaughan, R. Greg, and Peter W. Webley. "Satellite observations of a surtseyan eruption: Hunga Ha'apai, Tonga." *Journal of Volcanology and Geothermal Research* 198.1-2 (2010): 177-186.

Withers, Mitchell, et al. "A comparison of select trigger algorithms for automated global seismic phase and event detection." *Bulletin of the Seismological Society of America* 88.1 (1998): 95-106.

Zobin, V. M., C. Navarro, G. Reyes-Dávila, J. Orozco, M. Bretón, A. Tellez, G. Reyes-Alfaro, and H. Vázquez (2006), The methodology of quantification of volcanic explosions from broadband seismic signals and its application to the 2004–2005 explosions at Volcán de Colima, México, *Geophys. J. Int.*, **167**(1), 467– 478, doi:10.1111/j.1365-246X.2006.03108.x.

Zobin, Vyacheslav M., et al. "Scaling relationship for Vulcanian explosions derived from broadband seismic signals." *Journal of Geophysical Research: Solid Earth* 114.B3 (2009).

Supplementary materials

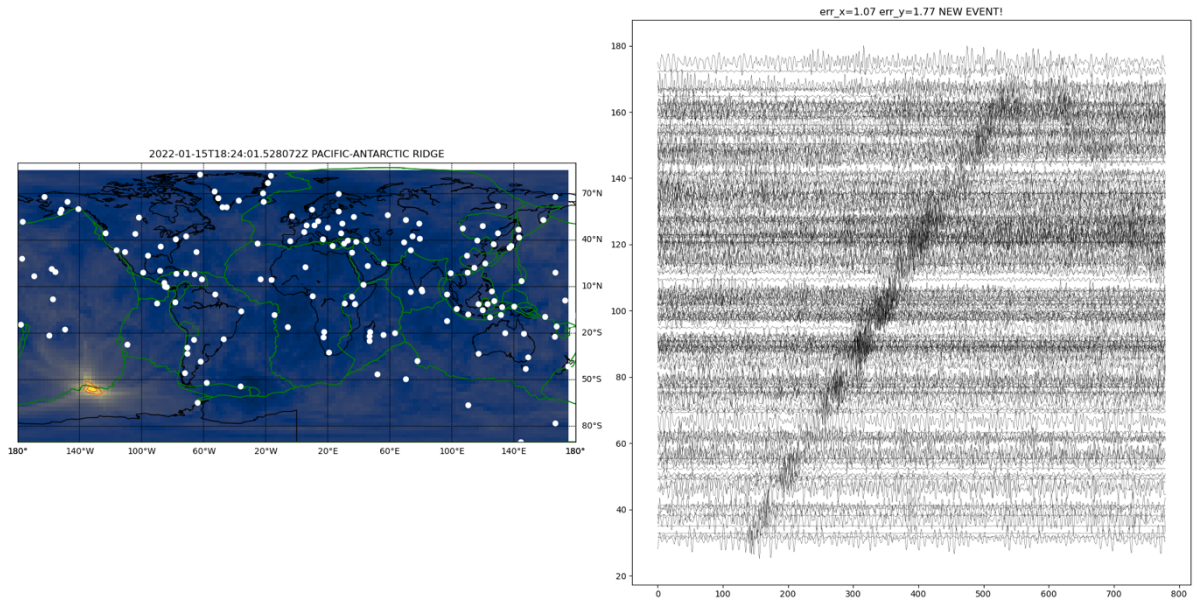

Fig S1: *New detection (event 5) for the 22 of January 2022. Left – map of the network stack at event time, Right – Detected signals as function of distance from the source.*

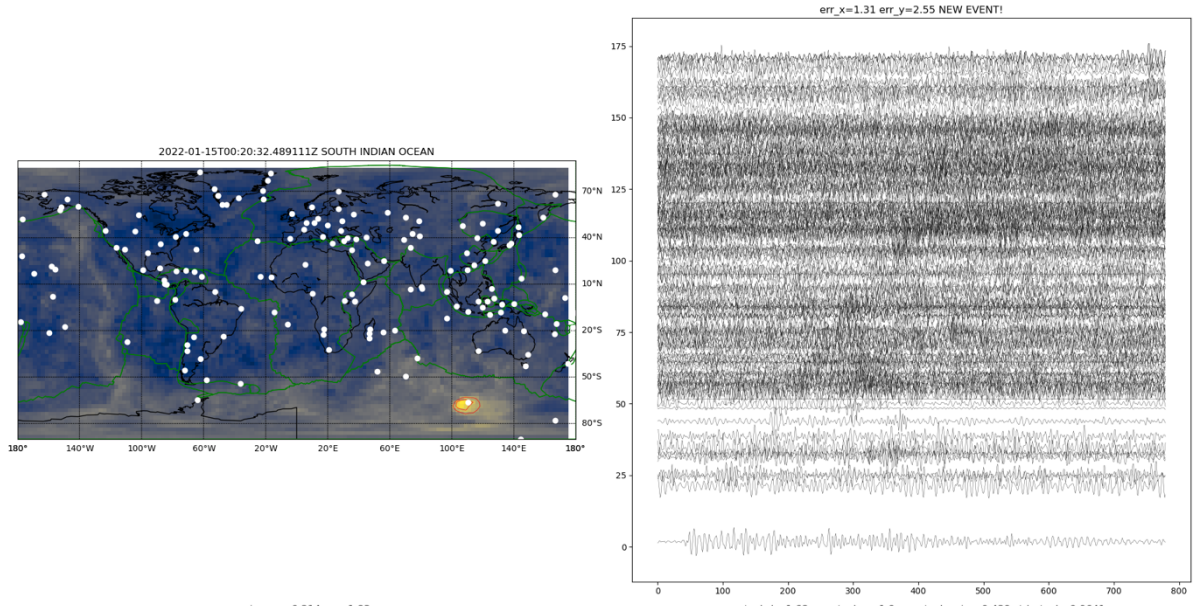

Fig S2: *New detection (event 6) for the 22 of January 2022. Left – map of the network stack at event time, Right – Detected signals as function of distance from the source.*

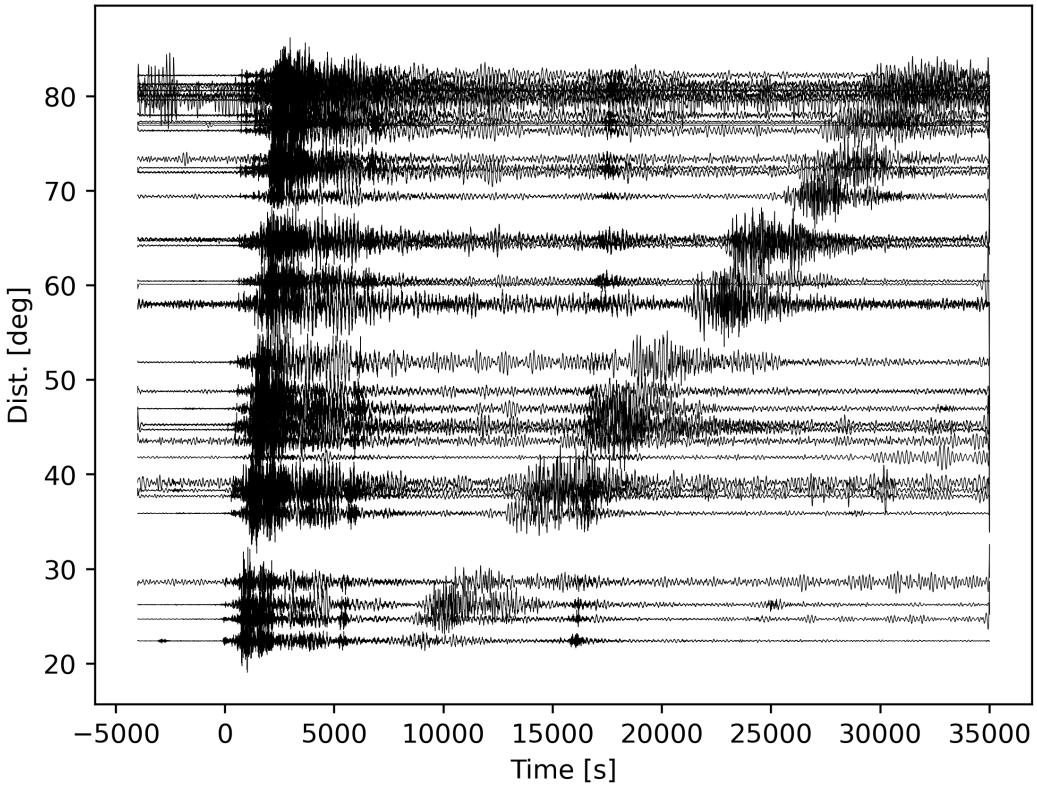

Figure S3: *Data used to study the explosion force filtered between 5mHz and 1Hz. Each seismogram is normalized by its amplitude maximum. The late slow arrival is the signature of the atmospheric acoustic waves generated by the Hunga Tonga eruption.*

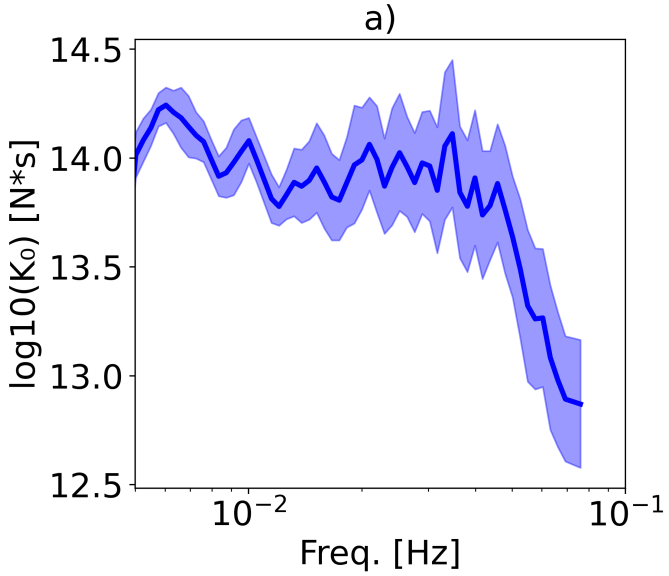

Figure S4: *Force spectrum estimated using only the first 1000s of surface waves.*